Simulating CO2 Storage in Saline Aquifers with Improved code RCB

SHUNPING LIU
Department of Physics and Technology
University of Bergen
Allégaten 55, No 55
Norway

BJORN KVAMME
Department of Physics and Technology
University of Bergen
Allégaten 55, Bergen
Norway

Abstract: - The geological storage of CO2 in saline aquifers is believed to be one of the most promising ways to reduce the concentration of the greenhouse gas in the atmosphere. Injection of CO2 will, however, lead to dissolution of minerals in regions of lowered pH and precipitation of minerals from transported ions in regions of higher pH. The geomechanical implications of these changes on the stability of the reservoir is of crucial importance in the evaluation of potential injection reservoirs. The possible injection rate for given over-pressures of the injected CO2 depends on the porosity and permeability of the rock matrix in the vicinity of the injection well. Local fracturing in this region can be a tool for increasing the injection flow rate but a geomechanical analysis will be needed in order to make sure that this fracturing will not affect the geomechanical stability outside this limited region to a significant degree. This paper presents a new application of improved code RCB (RetrasoCodeBright) to simulate CO2 storage in saline aquifer. According to specification of carbon dioxide under injecting, gas density and gas solubility have been corrected in code RCB. Newton-Raphson method used to solve the flow and mechanics in RCB has been improved so as to make the solutions always converge even under high gas injecting pressures. A 2D hydro-chemical-mechanical problem is solved by the original and the improved RCB code. The results are presented and compared.

Key-Words: - CO2, saline aquifer, RCB (RetrasoCodeBright), simulation, multiphase flow, geomechanics, geochemistry, gas density correction, gas solubility correction, improved Newton-Raphson iteration method, relaxation factor.

1 Introduction

The geological storage of greenhouse gas in deep saline aquifers can be one of the most promising options to reduce the concentration of CO2, the major greenhouse effect contributor, in the atmosphere [13]. Saline aquifers are water bearing porous layers of sandstone or limestone in the subsurface and by far they are the volumetrically largest, and widespread, proposition for large-scale CO2 storage. Several CO2 storage projects are at present active, i.e. the SACS project (Saline Aquifer CO2 Storage) initiated 1998 in North Sea Utsira Formation reservoirs [7]; the CO_2SINK project started in April 2004 at Ketzin in Germany have demonstrated the big potential of saline aquifers for long term CO2 deposits [14]. More geologically CO2 sequestration projects are planned to start in the near future.

To study the migration, transformation and to predict the ultimate long term fate of CO_2 injected, modeling tool that considers all the chemical species and their concentrations in minerals and liquid are required. And since ions are transported with the "bulk" flow, as well as internally in each volumetric block by diffusion it is necessary to couple the implications of chemical reactions to multi-phase models for flow of brine, CO2 gas and transport of solutes in liquid by means of advection and diffusion. Detailed geologically characterisations have not been taken into consideration when we are evaluating a numerical model used to solve this complex geomechanical-hydraulic-geochemical system.

Several modeling code for modeling these systems have been presented in recent years. One of them as finished in 2005, ATHENA/ACCRETE approach developed by the researchers in Department of Physics

and Technology and Department of Mathematics in University of Bergen have been chosen to for evaluation of the SACS project of CO2 from the Sleipner field into Utsira formation [7]. Reservoir simulator ATHENA is built on the SOM (secondary oil migration) platform and developed into a platform for analyses of CO2 migration over long time scales and long distances. But there are some limitations of this software that can not be neglected.

Firstly the reactive flow module in ATHENA is assuming that the reactions do not affect the fluid flow significantly except for trivial porosity/permeability changes as estimated from ”accepted” / common correlations. The CO2 Utsira formation contains only small amounts of quickly dissolving carbonates. But several relevant storage reservoirs contains much sandstone or limestone (calcite is the main chemical element), For reservoirs with much higher content of quickly dissolving minerals, these approximations are apparently not suitable. Secondly the huge and complicated platform of ATHENA makes it difficult to upgrade the code later on.

It is very necessary to develop a new modeling method capable to be used in more common situations. Aiming at solving this problem, project “Observing the effect of long term CO2 storage in saline aquifers” is carried out in Department of Physics and Technology in University of Bergen. And as the centre of the project, code RCB (RetrasoCodeBright) has been chosen to be the software platform. RCB is the result of coupling two codes: CodeBright and Retraso. CodeBright (COupled DEformation of BRIne Gas and Heat Transport) was designed for the thermo-hydraulic-mechanical analysis of three-dimensional multiphase saline media (Olivella et al., 1996; Departamento de Ingeniería del Terreno, 2002). Retraso (REactive TRAnsport of SOlutes) is a code for solving two-dimensional reactive transport problems (Saaltink et al., 1997) [4].

Relative to many other available reservoir modeling tools, the implicit algorithm for the geomechanical analysis is a distinction which makes this code attractive as a basis for development of a state of the art simulator for CO2 storage scenarios. RCB code contains many significant features [4]. It is developed on the foundation of geomechanical simulation’s code CodeBright. Unlike the few other codes worldwide which also has been extended with a geomechanical analysis “on top” Code Bright has very advanced geomechanical models which also able to analyse complex non-rigid geomechanical behavior like the one we might expect during outdrying and potential empbrittlement of shale and clay in the cap rock zones.

Basically, in the coupled code RCB, a CodeBright module calculates the flow properties (Darcy flux of liquid and/or gas, saturation, temperature, density, displacements, etc.) and passes it to a Retraso module for the calculation of reactive transport and impact of geochemistry on the fluid flow [4][5]. Both parts will be sequentially finished calculating in one time step. All the solutions from last time step will be the corresponding parameters sent to the iteration of next time step. Following figures shows the procedure:

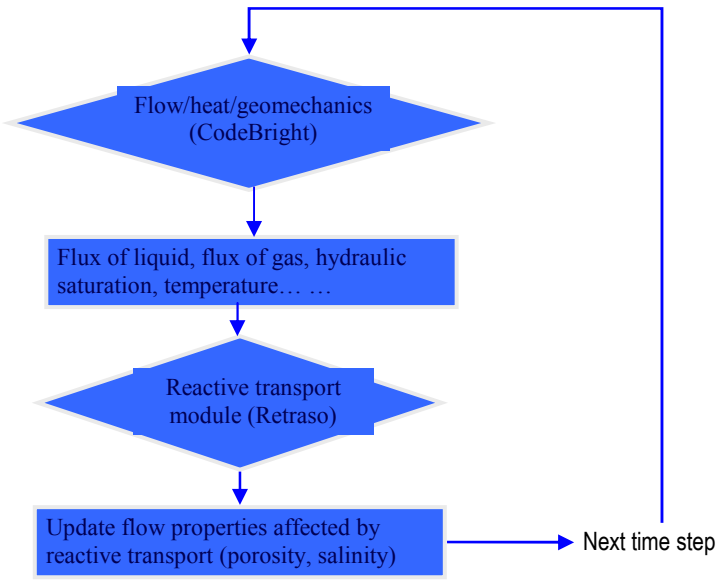

Fig. 1 RCB solves the integrated equations sequentially in one time step.

The mathematical equations for the system are highly non-linear and they will be solved numerically [5]. The numerical approach can be viewed as divided into two parts:

spatial and temporal discretizations. Finite element method is used for the spatial discretization while finite differences are used for the temporal discretization. The discretization in time is linear and the implicit scheme uses two intermediate points, $t^{k+\varepsilon}$ and $t^{k+\theta}$ between the initial t^k and final t^{k+1} times. The Newton-Raphson method is adopted to find an iterative scheme [2] [3].

RCB is a very advanced module for flow, heat, geomechanics and geochemistry calculation [1] [2]. Moreover, it has offered possibilities of just computing the chosen unknowns according to user if there are just a part of these unknowns are interested. For instance: hydro-mechanical, thermo-mechanical, hydro-thermal, hydro-chemical-mechanical, hydro-thermal-chemical-mechanical problems can be solved if the physical situation requires one of these approaches. Geometrically, RCB can handle problems in different dimensions, i.e. 1D, 2D and 3D [3].

Due to these positive features, we have chosen RCB as the new module to simulate and evaluate CO2 storage in saline aquifers. But unfortunately the original RCB code can not be used directly for our purpose because 1) the geochemical part of this package is essentially EQ36 but present version assumes ideal gas which is far from the reality; 2) solutions don't converge in the Newton-Raphson iteration scheme if CO2 injection pressure is higher than around 55 bars. In fact, CO2 is injected under be a super-critical fluid conditions at Utsira about 120 bars[7]. So adding improvement to the original RCB code is absolutely necessary.

In this paper, RCB code is improved by doing three main corrections in implementation. The first two are the corrections for fugacity coefficients and Poynting corrections in the gas (CO2)/liquid equilibrium respectively in CodeBright part and Retraso part [6]. These corrections are essentially straightforward to implement. The third correction is the density correction in the gas flow equations. These corrections also essentially straightforward give that the compressibility factors are known [16]. The other optimization is done by modifying the conventional Newton-Raphson method which introduces a relaxation factor α to make the iterative process converge faster. In their inspiring paper [8] T. Nakata and K. Fujiwara show various methods searching for the relaxation factors. We develop the algorithm to get the proper relaxation factor in RCB code by combining the general tendency method [8] and time step reduction method. This method manages to make the iterative process definitely converge no matter how high the injecting pressure is.

To compare the effects of unchanged and changed RCB code, a specific 2D hydro-chemical-mechanical example is examined by the original RCB code and the improved RCB code. The consequent results of some important hydraulic, mechanical and chemical features are put together in graphic window GiD [15].

2 Modifications in RCB code

2.1 Gas density correction

The gas phase in the original RCB is assumed to be at quite low pressures and behaves as ideal gas which obeys the ideal gas equation:

$$PV = nRT \tag{1}$$

This approximation will be failed in reality. We rewrite the gas equation as:

$$PV = ZnRT \tag{2}$$

where Z is the compressibility factor for the gas. Compressibility factor Z for CO2 is calculated using the SRK EOS tabulated as function of temperature T and pressure P and estimated by bilinear interpolation [6]. We can write the concentration of CO2 in gas phase (c_{co2}), expressed in mole per unit of volume, as:

$$c_{co2} = \frac{P}{ZRT} \tag{3}$$

And we can get the gas density of CO2 as:

$$\rho_{co2} = \frac{PM_{CO2}}{ZRT} \quad (4)$$

where P is pressures in bar, M_{CO2} is molar weight of CO2 (44.01 g/mol), R is the gas constant (8.3143 $J \cdot K^{-1} \cdot mol^{-1}$) and T is temperature in Kelvin.

Partial derivative of CO2 density with pressure at constant temperature is expressed as:

$$\left(\frac{\partial \rho_{CO2}}{\partial P}\right)_T = \frac{1}{Z \cdot RT} \cdot \left\{1 - P\left(\frac{\partial Z}{\partial P}\right)_T\right\} \quad (5)$$

where $\left(\frac{\partial Z}{\partial P}\right)_T = \frac{Z(T_x, P_2) - Z(T_x, P_1)}{P_2 - P_1}$, 1 or 2 is the subscripts address the table position in the Z *(T, P)* table.

2.2 Solubility of CO2

The bubblepoint mole fraction of CO2 is calculated according to:

$$x_{co2}^b = \frac{P\phi}{H_{co2}} \exp\left\{\frac{\overline{v}^{\infty}}{RT}(1 - P)\right\} \quad (6)$$

where ϕ is the fugacity coefficient for CO2 estimated from the SRK equation of state, *H* is the
Henrys law coefficient for CO2, *P* is pressure (bar), *T* is temperature (K), *R* is the gas constant, and $\overline{v}^{\infty}$ is the partial molar volume of CO2 at infinite dilution. The fugacity coefficient is calculated as a function of temperature and pressure by a polynomial that is interpolated from SRK data. Similarly is the Henrys law coefficient found from a polynomial that is interpolated as a function of temperature and salinity from listed experimental data in [6]. The exponential term in equation (6) is the Poynting correction to the Henrys law coefficient.

2.3 Modifying Newton-Raphson scheme in CodeBright

When nonlinear hydro- mechanics system is analyzed by using the conventional Newton-Raphson method, the iterative process often fails to provide convergent solutions [9][10]. It is the reason why when boundary CO2 injecting pressure is higher than 55 bar, iteration in the old RCB code can not manage to carry on.

The governing equations for non-isothermal multiphase flow of liquid and gas through porous deformable saline media have been established by Olivella et al. (1994). Variables and corresponding equations are tabulated as the following:

Equation	Variable name	Variable
Equilibrium of stresses	Displacements	u
Balance of liquid mass	Liquid pressure	Pl
Balance of gas mass	Gas pressure	Pg
Balance of internal energy	Temperature	T

Table1. Equations and variables

After the spatial discretization of the partial differential equations, the residuals that are obtained can be written (for one finite element) as:

$$\begin{pmatrix} r_u \\ r_{Pl} \\ r_{Pg} \\ r_T \end{pmatrix} = \frac{d}{dt}\begin{pmatrix} d_u \\ d_{Pl} \\ d_{Pg} \\ d_T \end{pmatrix} + \begin{pmatrix} a_u \\ a_{Pl} \\ a_{Pg} \\ a_T \end{pmatrix} + \begin{pmatrix} b_u \\ b_{Pl} \\ b_{Pg} \\ b_T \end{pmatrix} = \begin{pmatrix} 0 \\ 0 \\ 0 \\ 0 \end{pmatrix} \quad (7)$$

where **r** are the residuals, *d***d**/*dt* are the storage or accumulation terms, **a** are the conductance terms, and **b** are the sink/source terms and boundary conditions. After time discretization a more compact form can read as:

$$r\left(X^{k+1}\right) = \frac{d^{k+1} - d^k}{\Delta t^k} + A\left(X^{k+\varepsilon}\right)X^{k+\theta} + b\left(X^{k+\theta}\right) = 0 \quad (8)$$

where *k* is the time step index, :
$\mathbf{X}=[(ux,uy,uz,Pl,Pg,T)_{(1)}, ..., (ux,uy,uz,Pl,Pg,T)_{(n)}]$, is the vector of unknowns (i.e. a maximum of seven degrees of freedom per node), **A** represents the conductance matrix. The Newton-Raphson scheme of solution for this non-linear system of
AE's is:

$$\frac{\partial r\left(X^{k+1}\right)}{\partial X^{k+1}}\left(X^{k+1,l+1}-X^{k+1,l}\right)=-R\left(X^{k+1,l}\right) \quad (9)$$

where l indicates iteration. In the present approach, the standard Galerkin method is used with some variations in order to facilitate computations.

If the optimum relaxation factor α_m [11], which minimizes the total square residual for the Galerkin method, is introduced at each step of the nonlinear iteration, convergent solution can be always obtained [11]. However, it takes very long time to find to find α_m, because a large number of repeating calculations of square residual is required.

The relaxation factor is determined so that the objective function $W^{(k+1)}$ at the (k+1)-th step of the nonlinear iteration is less than $W^{(k)}$ at the previous step as follows:

$$W^{(k+1)} < W^{(k)} \quad (10)$$

The relaxation factor which satisfies (10) is searched for by using the following equation:

$$\alpha^{(k)} = 1/2^n \qquad (n = 0,1,...,i) \quad (11)$$

When (10) is satisfied, the calculation of (11) changing n is determined at $n = i$.

3 A 2D hydro-chemical-mechanical example

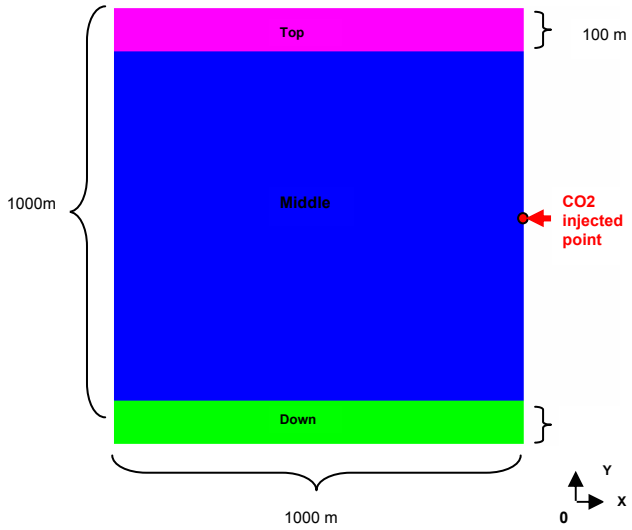

Fig.2 Geometry of the 2D reservoir and the CO2 injecting point

The geometry of this 2D domain is a 1000 m x 1000 m square. There are two different kinds of geological structures in the whole domain as illustrated with two different colors. The pink zone (Top) and green zone (Down) has the same geological structure. And the blue zone (Middle) has different geological structure. Each of “Top” and ”Down” zones is a 1000m x 100m rectangular; while the blue zone is a 1000m x 800m rectangular. CO2 is injected into the middle point of the right boundary.

Initially, there is fine grained sand of pure calcite and its saturate solution in the “Middle” zone. In “Top” and “Down” zones, there are fine grained sand of 3% calcite and 97% quartz. The CO2 injecting pressure is 120 bar. Temperature does not change in the whole process. It is kept 25 Celsius in the whole area from the injection started.

The initial liquid pressure and gas pressure in the 2D reservoir are respectively 50 bar and 30 bar. Except the boundary on the left side, neither liquid nor gas can infiltrate through other boundaries. Except the boundary on the right side, every boundary has displacements restriction. It is assumed that there are no initial displacements and no

initial stress in the whole area.

The simulation time is 100 years.

4 Results and Discussions

The simulation results for hydraulic, mechanic movements and chemical transport in the 2D saline aquifer processed by improved RCB code can be visualized in GiD window [15]. Six evolution time points have been chosen at which some important features describing the changing in geometry, liquid and gas transport are illustrated for that CO2 is treated as ideal gas and a real fluid with gas density correction and CO2 solubility correction. Result of the comparison is attached in Appendix 1.

Keeping in mind that the flow is driven by a constant difference in the injection pressure and the pressure on the left side of the model formation there are some properties which will not be very much affected by the transition from ideal gas to real gas description. Dissolution of calcite carbonate, the rapidly dissolving mineral, in the low pH regions leads to a buffering effect due to released carbonate ions that shifts the dissolution reactions towards less dissolved CO2. But the ions are transported with the reservoir fluid flow and the question is the balance between the buffering and the erosion due to dissolved carbonates and ion transport away from the vicinity of the injection region. The most pronounced effects are in the dissolved gas and corresponding pH, in which the buffering effect is very clear. The increased buffering in the real gas case results in significantly higher pH values for the real gas case. But for both cases the pH remains above 5 in all regions and the corresponding effects on erosion is limited for ideal gas case as well as real gas case. Within the simulated period the effects on porosity and stress is very limited for this special example.

The contrast of dissolved CO2 gas in liquid between the situation of CO2 as ideal gas and CO2 as non-ideal fluid illustrates that ideal gas dissolves more easily due to the buffering effect.

The corrected version of the has been applied to a simple test case containing an inner section (80%) of pure calcite and two equal section of quartz (97%) and calcite. As expected the buffering effect is substantial during the maximum simulation time of 100 years. For this specific example the erosion and corresponding geomechanical instability effects are very limited for the actual injection rates.

5 Conclusions

We have extended a geomechanical reactive transport simulator RetrasoCodeBright into high pressures relevant for reservoir storage of CO2. Corrections for non-ideal gas has so far been based upon the SRK equation of state but can easily be replaced by similar results from any equation of state since the necessary data are interpolated from calculated tables of compressibility factors and fugacities as function of temperature and pressure. In addition the convergence of the Newton-Raphson iterative solution has been improved through implementation of an algorithm that minimizes the total square residual for the Galerkin method after each Newton-Raphson step. The corrected version has been applied to a simple test case with high buffering effect (a dominating section of pure calcite). For the particular test case the erosion is very limited and the corresponding geomechanical implications of the CO2 injection estimated to be correspondingly small, even for time periods up to 100 years.

References:

[1] Olivella, S., J. Carrera, A. Gens, E.E. Alonso, “Non-isothermal Multiphase Flow of Brine and Gas through Saline Media”, Transport in Porous Media, 15, pp. 271-293, 1994

[2] Olivella, S., A. Gens, J. Carrera, E. E. Alonso, “Numerical Formulation for a Simulator (CODE_BRIGHT) for the Coupled Análisis of Saline Media”, Engineering Computations, vol. 13, No.7, pp.87-112, 1996

[3] Olivella, S., A. Gens, J. Carrera, CodeBright User’s Guide. Barcelona, E.T.S.I. Caminos, Canales y Puertos, Universitat Politecnica de Catalunya and Instituto de Ciencias de la Tierra, CSIS, 1997

[4] Saaltink, M., Benet, I., Ayora, C., RETRASO, Fortran Code for Solving 2D Reactive Transport of Solutes, Users´s guide. Barcelona, E.T.S.I. Caminos, Canales y Puertos, Universitat Politecnica de Catalunya and Instituto de Ciencias de la Tierra, CSIC, 90 pp. 1997

[5] Saaltink, M., Batlle, M., Ayora, C., “RETRASO, a code for modeling reactive transport in saturated and unsaturated porous media”, Geologica Acta, Vol.2, No 3, pp. 235-251, 2004

[6] HELLEVANG, H. & KVAMME, B. “CO2-waterrock interactions - ACCRETE simulations geological storage of CO2”, Appl. Geoch., 2006

[7] H. Hellevang, S. K. Khattri, G. E. Fladmark and B. Kvamme. CO2 storage in the Utsira Formation: ATHENA 3-D reactive transport simulations, Submitted to the journal of Basin Research, 2005.

[8] T. Nakata and K. Fujiwara, “Method for determining relaxation factor for modified Newton-Raphson method”, IEEE TRANSACTIONS ON MAGNETICS, vol. 29, No. 2, MARCH 1993

[9] T. Nakata, N. Takahashi, K. Fujiwara, P. Olszewski and K. Muramatsu, "Analysis of magnetic fields of 3-D non-linear magnetostatic model (Problem 13)," Proceedings of the European TEAM Workshop and International Seminar on Electromagnetic Field Analysis, pp. 107-1 16, 1990.

[10] T. Nakata and K. Fujiwara, "Summary of results for benchmark problem 13 (3-D nonlinear magnetostatic model)," COMPEL, James & James, vol.11, 1992, in press.

[11] T. Nakata, N. Takahashi, K. Fujiwara, N. Okamoto and K. Muramatsu, "Improvements of convergence characteristics of Newton-Raphson method for nonlinear magnetic field analysis," IEEE Trans Magn., vol. M 28, no.2, pp. 1048-1051, March 1992.

[12] R. Albanese and G. Rubinacci, "Numerical procedures for the solution of nonlinear electromagnetic problems," ibid., vol. MAG-28, no.2, pp. 1228-1231, March 1992.

[13] R Stuart Haszeldine, “Deep geological CO2 storage: principles reviewed, and prospecting for bioenergy disposal sites”, http://www.accstrategy.org/simiti/Haszeldine.pdf

[14] CO2SINK, a research project of CO2 storage in underground geological formation in Ketzin, Germany, http://www.co2sink.org/

[15] CIMNE, International Center For Numerical Methods and Engineering, “GiD – The personal pre- and post processor”, http://gid.cimne.upc.es/

[16] Soave, G., “Equilibrium constants from a modified Redlich-Kwong equation of state” Chem. Eng. Sci., 27,1197-1203, 1972.

Appendix 1

Gas phase flux

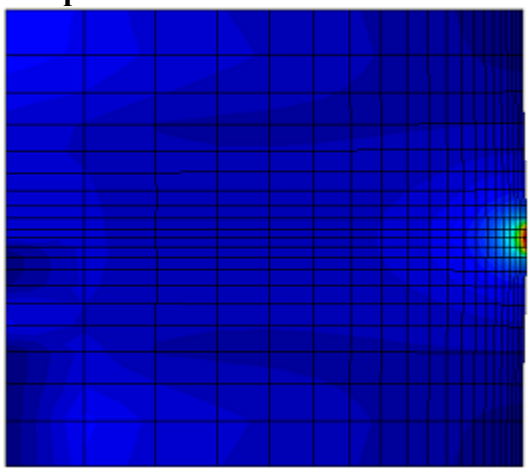

3a

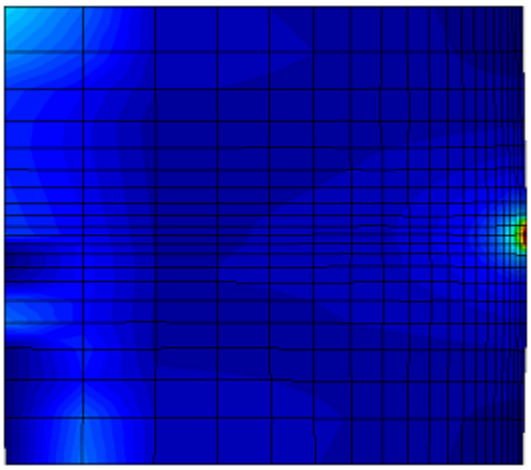

3a'

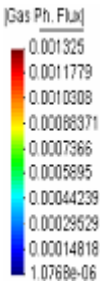

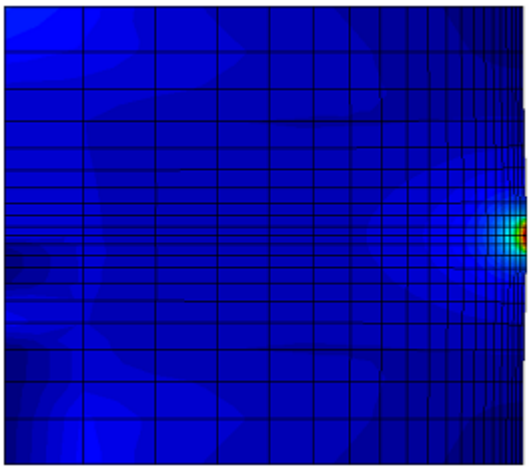

3b

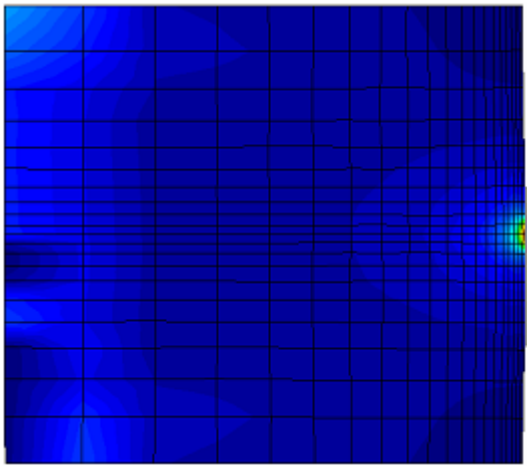

3b'

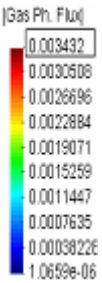

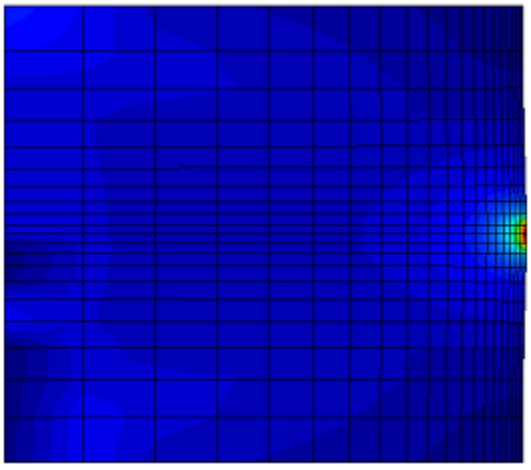

3c

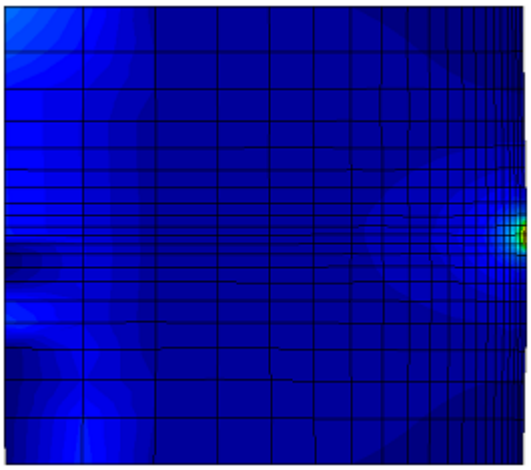

3c’

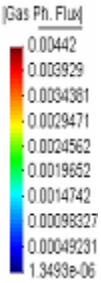
|Gas Ph. Flux|
0.00442
0.003929
0.0034381
0.0029471
0.0024562
0.0019652
0.0014742
0.00098327
0.00049231
1.3493e-06

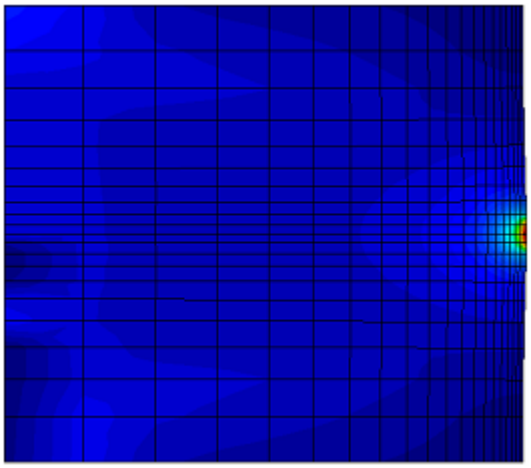

3d

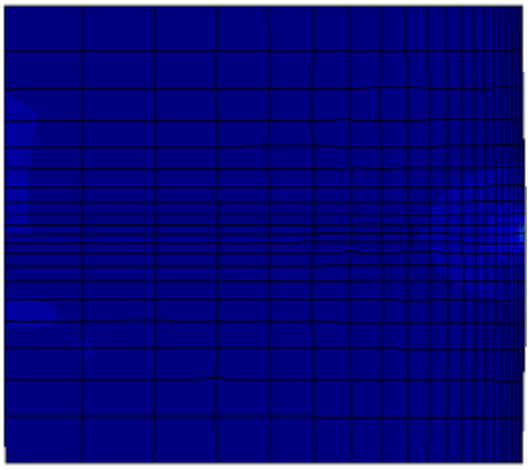

3d’

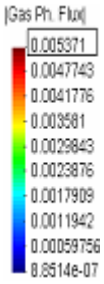
|Gas Ph. Flux|
0.005371
0.0047743
0.0041776
0.003581
0.0029843
0.0023876
0.0017909
0.0011942
0.00059756
8.8514e-07

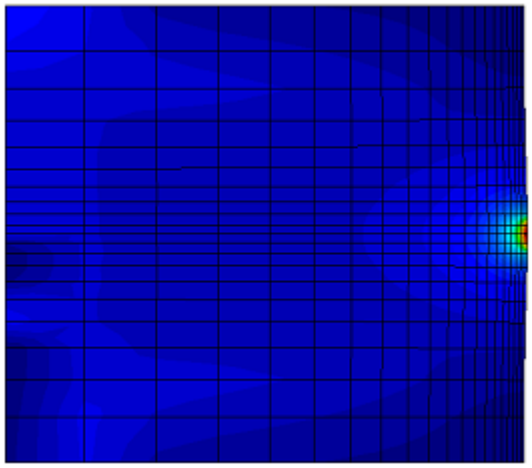

3e

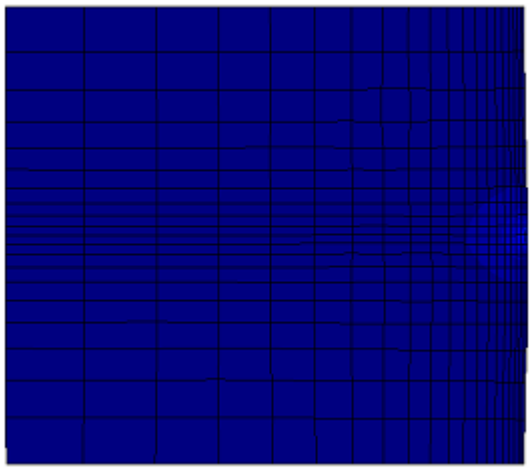

3e’

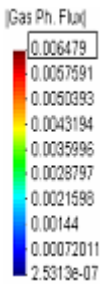
|Gas Ph. Flux|
0.006479
0.0057691
0.0050393
0.0043194
0.0035996
0.0028797
0.0021598
0.00144
0.00072011
2.5313e-07

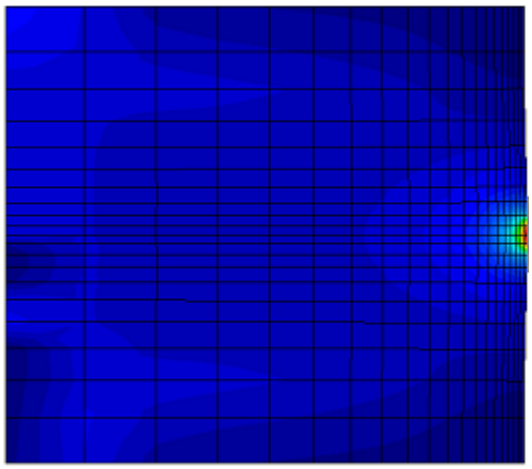

3f

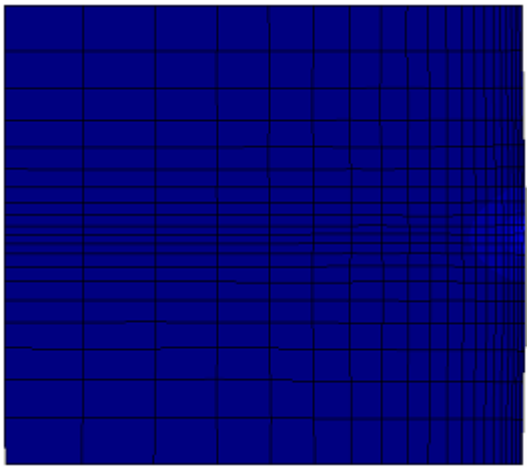

3f'

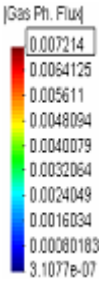

Fig.3 Plotted simulated results of gas phase flux ($kg.m^{-2}.s^{-1}$) at the time points of 1 year, 5 years, 10 years, 20 years, 50 years and 100 years after CO2 injected as ideal gas (the first) and as real fluid (the second).

Gas pressure

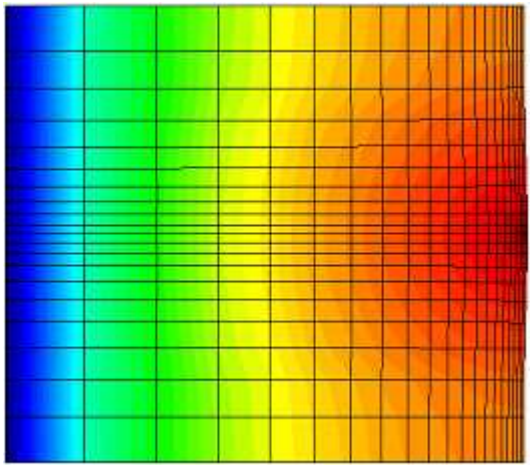

4a

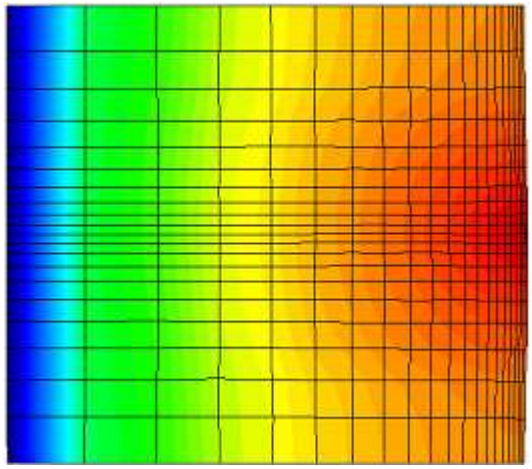

4a'

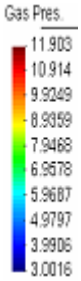

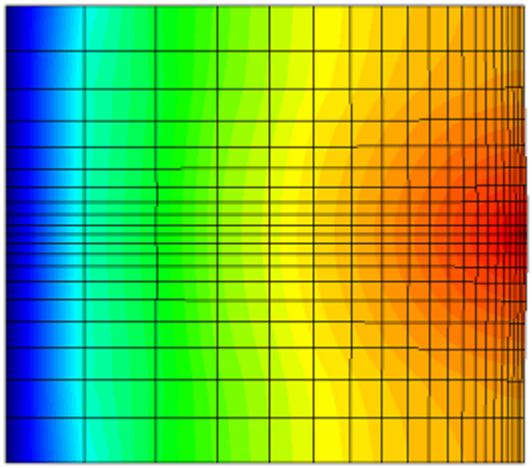

4b

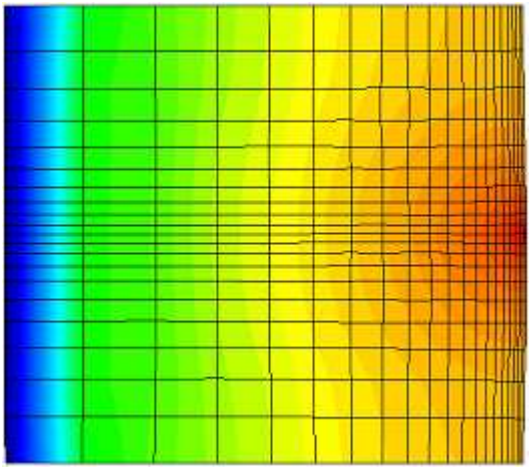

4c’

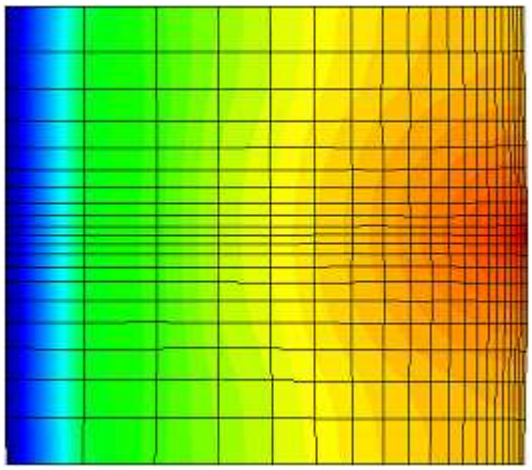

4b’

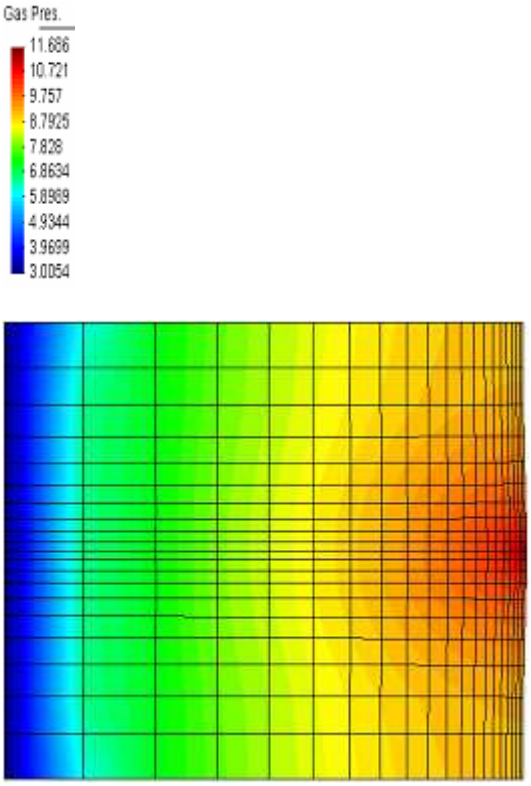

4d

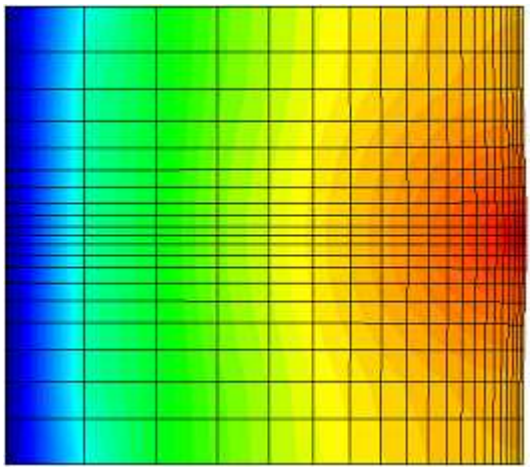

4c

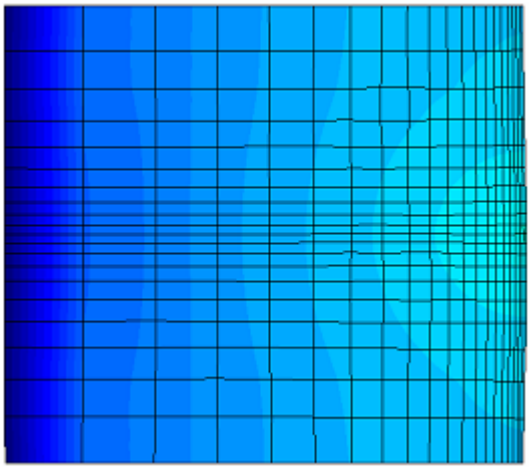

4d’

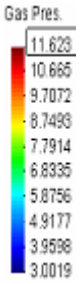

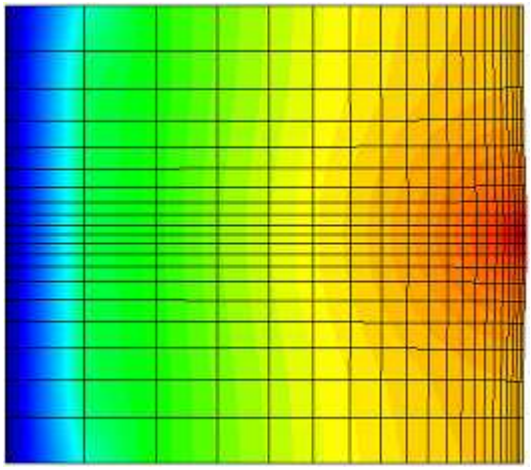

4e

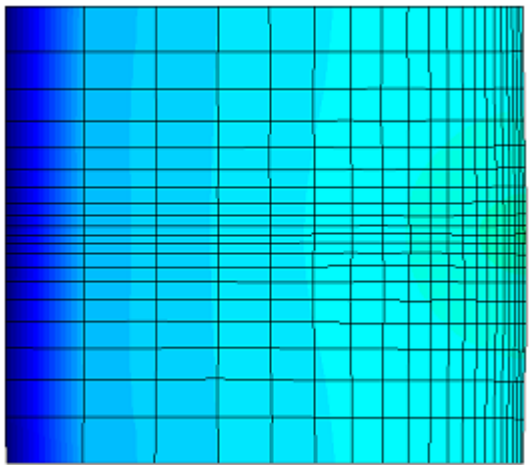

4e’

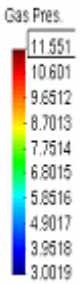

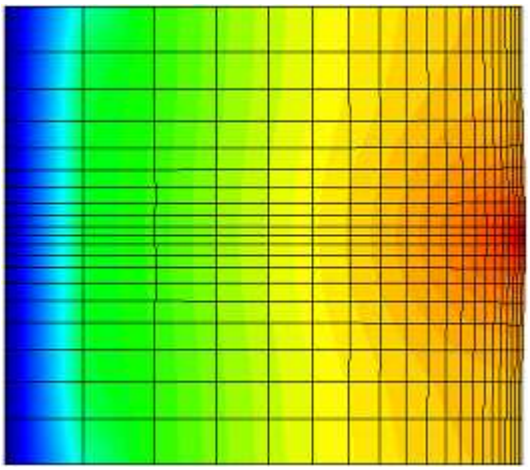

4f

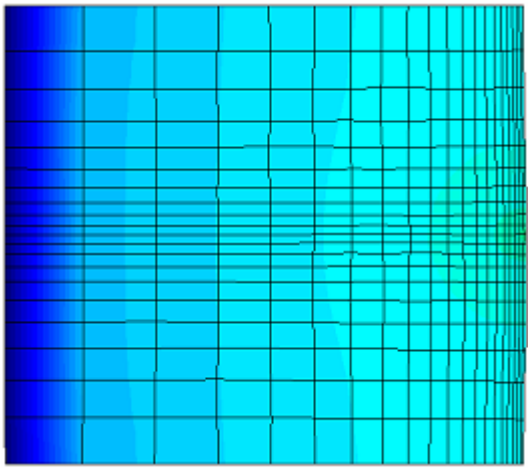

4f’

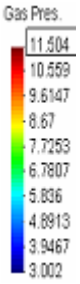

Fig.4 Plotted simulated results of gas pressure (MPa) at the time points of 1 year, 5 years, 10 years, 20 years, 50 years and 100 years after CO2 injected as ideal gas (the first) and as real fluid (the second).

Gas Density

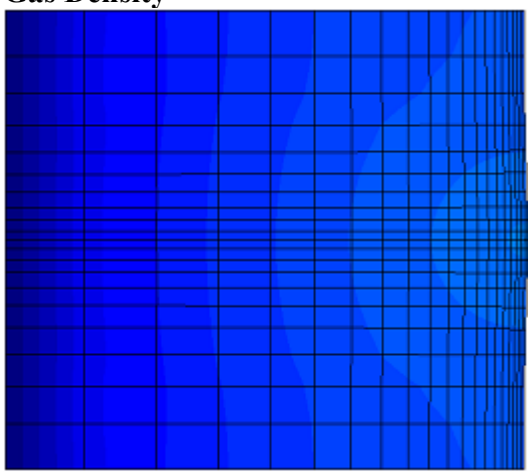

5a

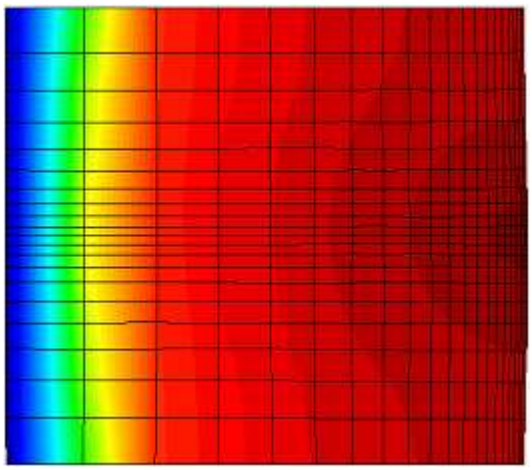

5a'

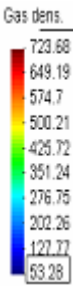

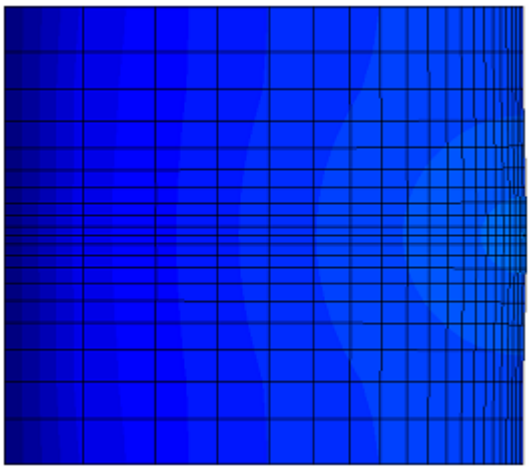

5b

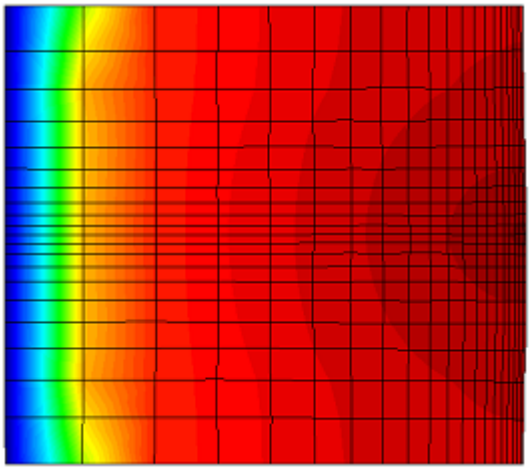

5b'

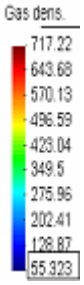

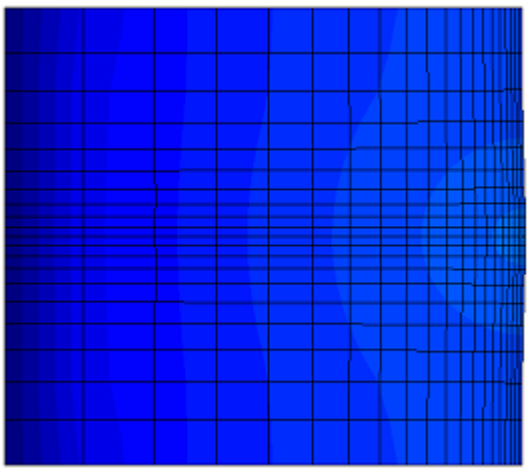

5c

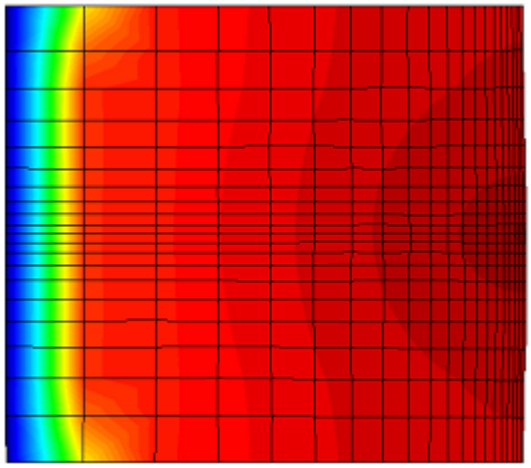

5c’

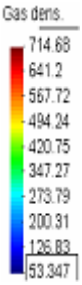
Gas dens.
714.68
641.2
567.72
494.24
420.75
347.27
273.79
200.31
126.83
53.347

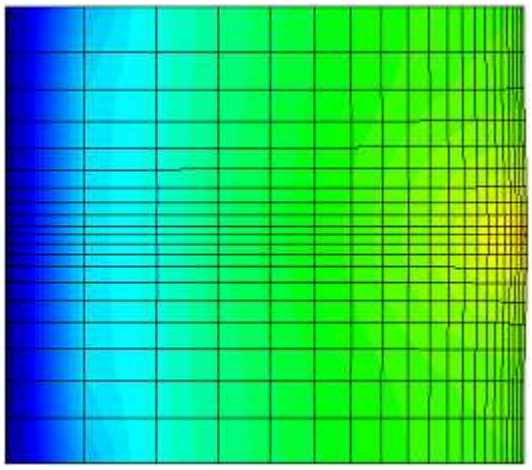

5d

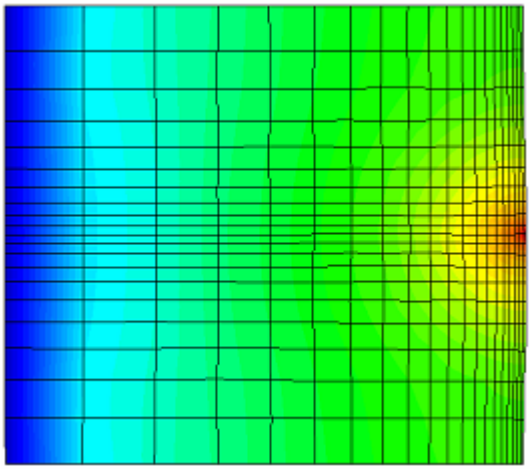

5d’

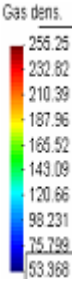
Gas dens.
255.25
232.82
210.39
187.96
165.52
143.09
120.66
98.231
75.799
53.368

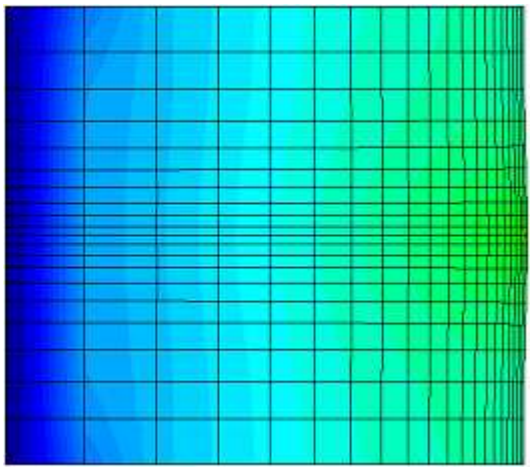

5e

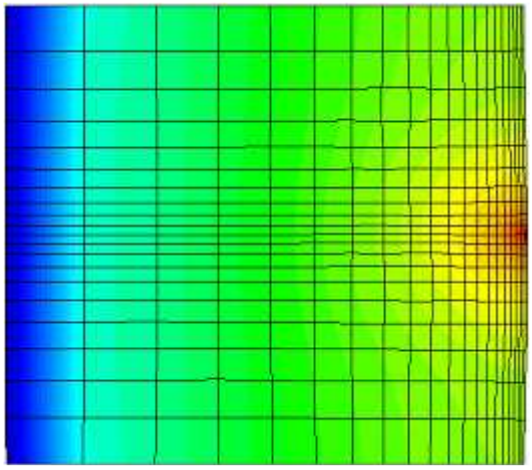

5e’

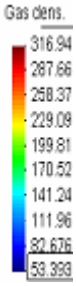
Gas dens.
316.94
287.66
258.37
229.09
199.81
170.52
141.24
111.96
82.676
53.393

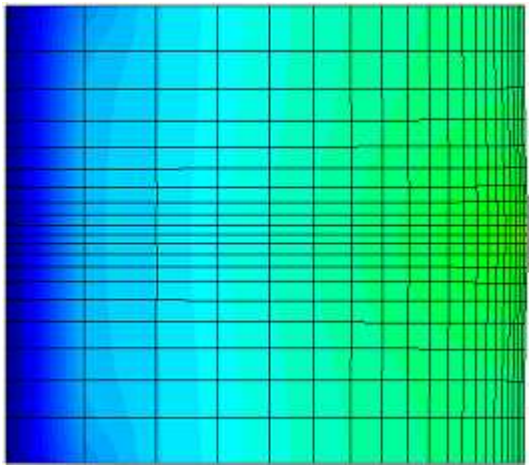

5f

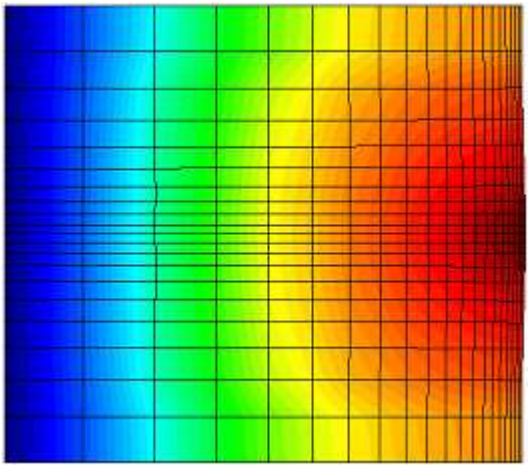

6a

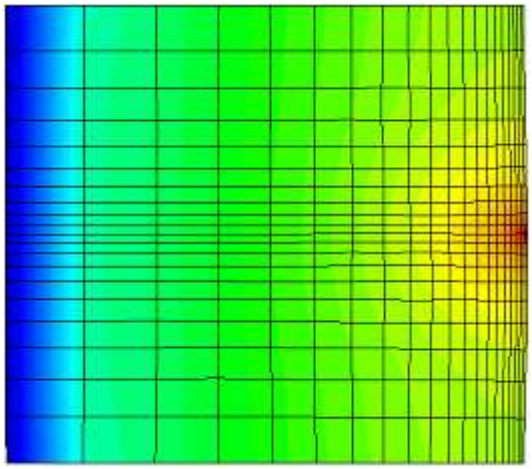

5f'

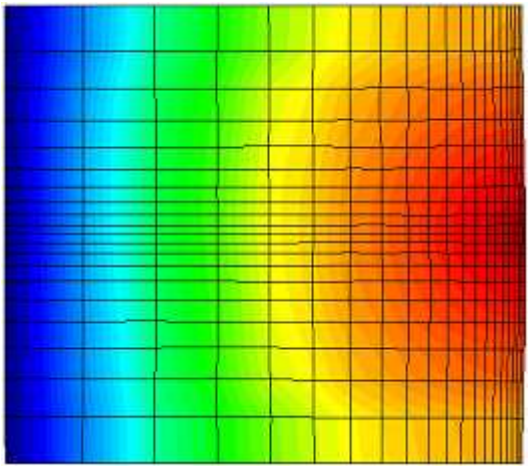

6a'

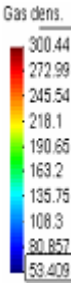

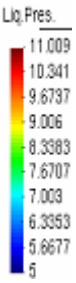

Fig.5 Plotted simulated results of gas density ($kg.m^{-3}$) at the time points of 1 year, 5 years, 10 years, 20 years, 50 years and 100 years after CO2 injected as ideal gas (the first) and as real fluid (the second).

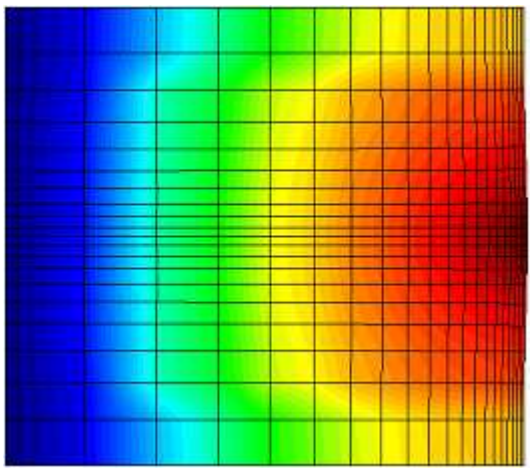

6b

Liquid Pressure

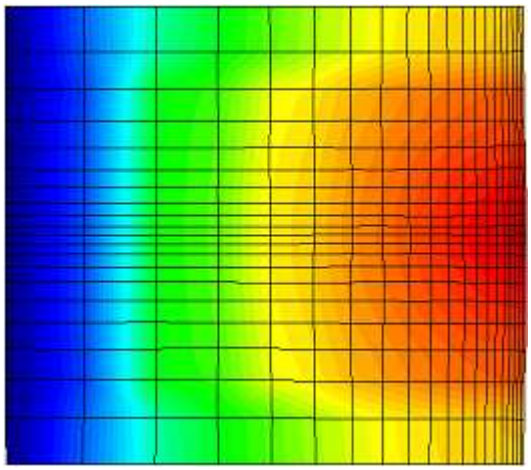

6b’

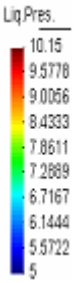
Liq.Pres.
10.15
9.5778
9.0056
8.4333
7.8611
7.2889
6.7167
6.1444
5.5722
5

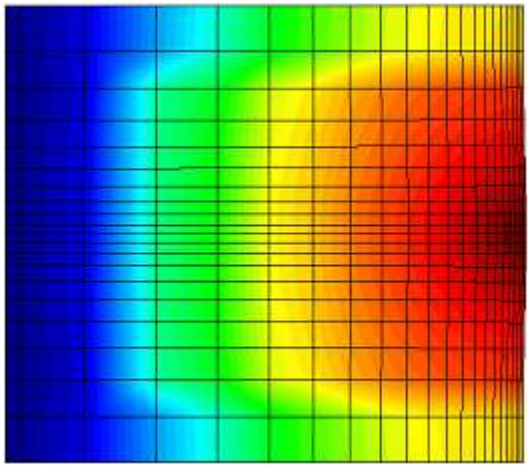

6c

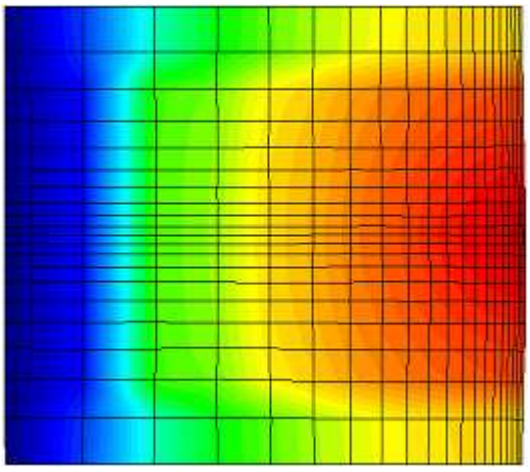

6c’

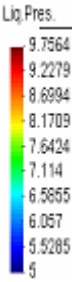
Liq.Pres.
9.7564
9.2279
8.6994
8.1709
7.6424
7.114
6.5855
6.057
5.5285
5

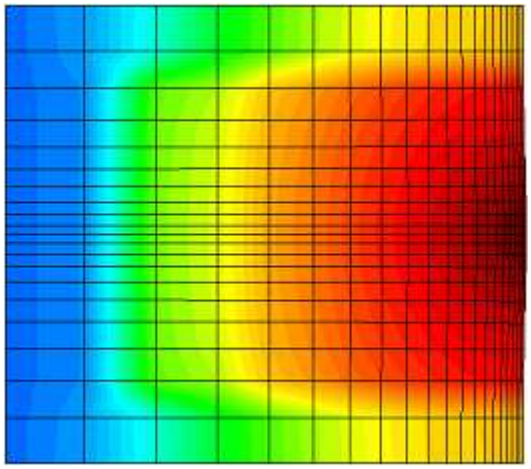

6d

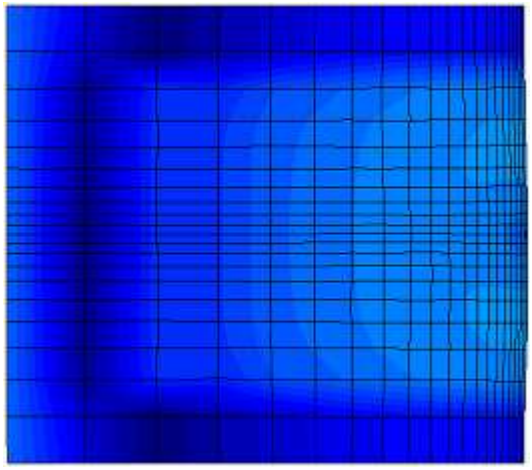

6d’

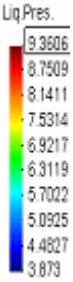
Liq.Pres.
9.3606
8.7509
8.1411
7.5314
6.9217
6.3119
5.7022
5.0925
4.4827
3.873

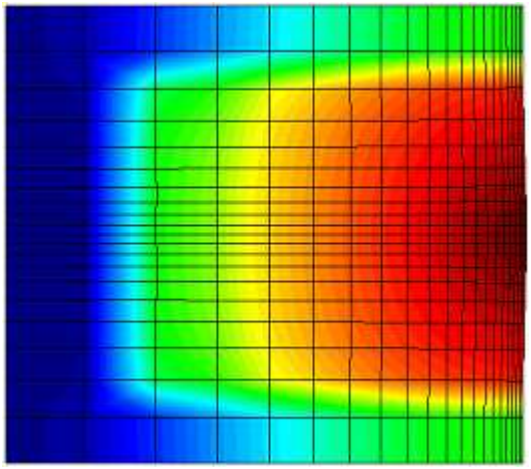

6e

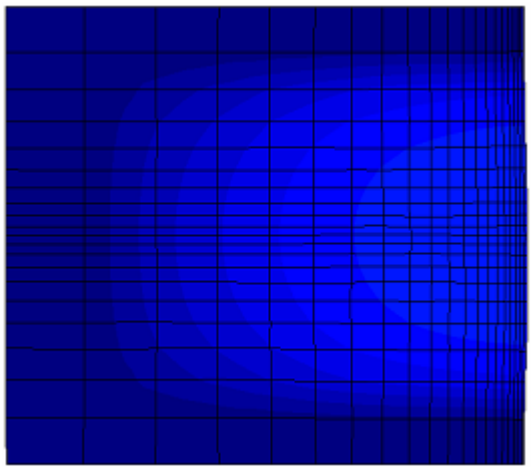

6e'

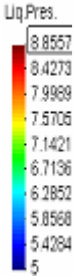

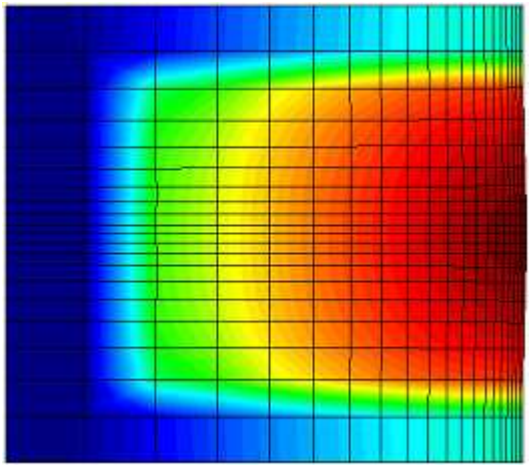

6f

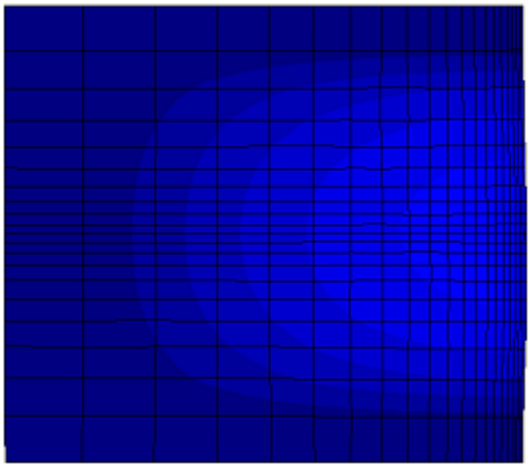

6f'

Fig.6 Plotted simulated results of liquid pressure (MPa) at the time points of 1 year, 5 years, 10 years, 20 years, 50 years and 100 years after CO2 injected as ideal gas (the first) and as real fluid (the second).

Liquid saturation

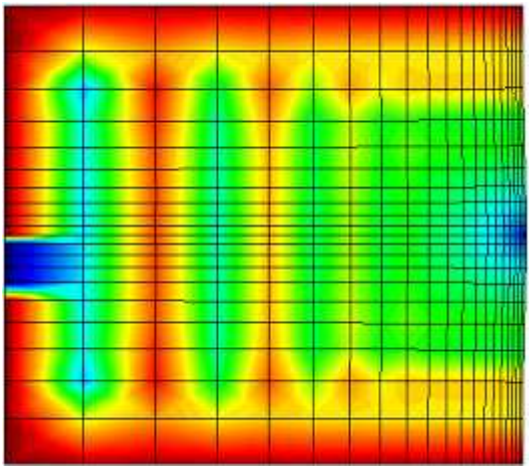

7a

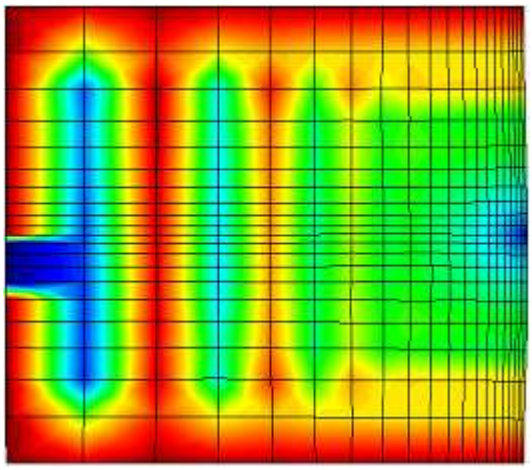

7a’

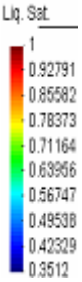
Liq. Sat.
1
0.92791
0.85582
0.78373
0.71164
0.63956
0.56747
0.49538
0.42329
0.3512

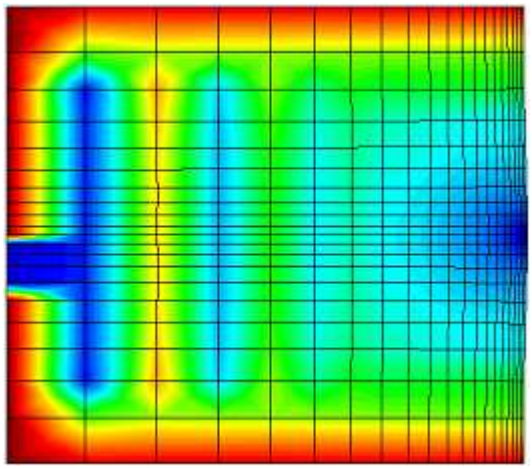

7b

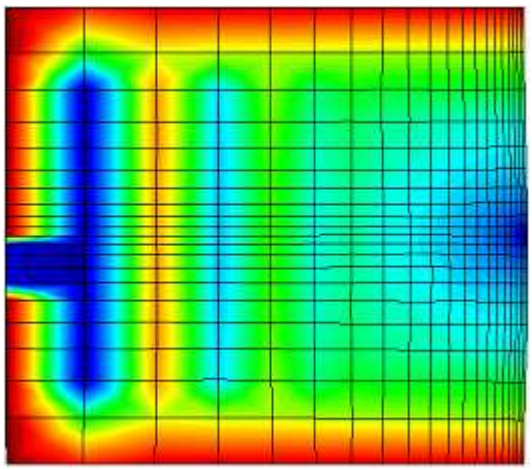

7b’

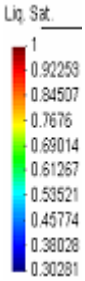
Liq. Sat.
1
0.92259
0.84507
0.7676
0.69014
0.61267
0.53521
0.45774
0.38028
0.30281

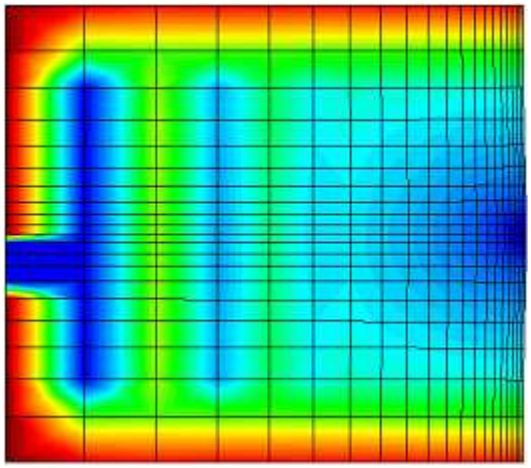

7c

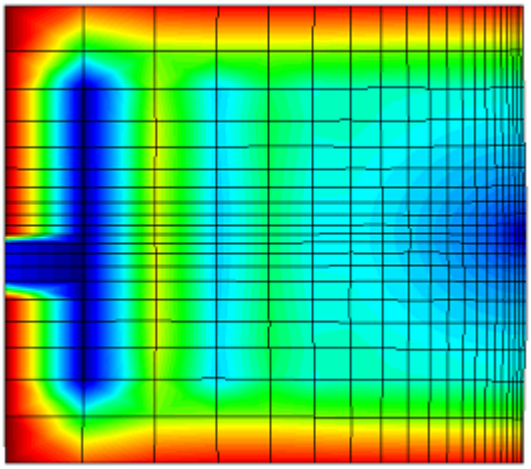

7c’

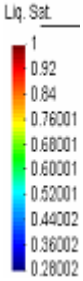
Liq. Sat.
1
0.92
0.84
0.76001
0.68001
0.60001
0.52001
0.44002
0.36002
0.28002

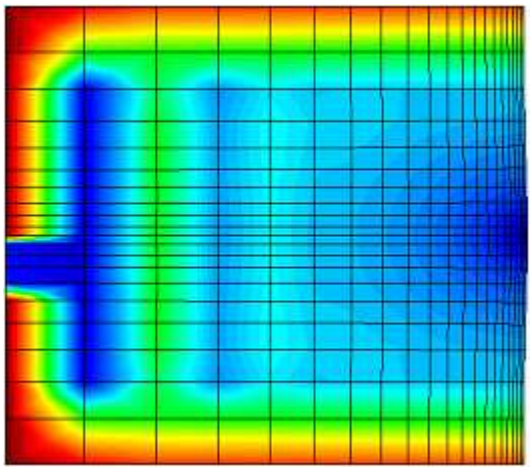

7d

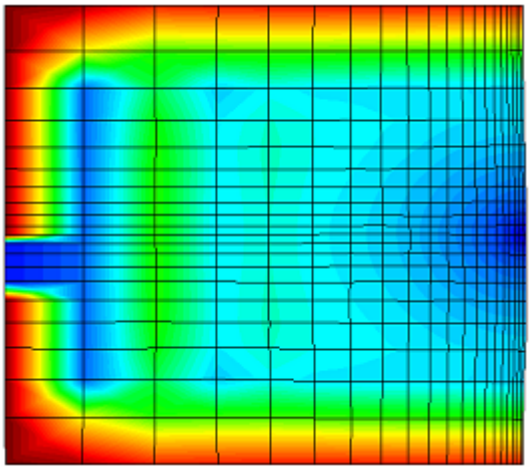

7d'

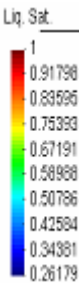

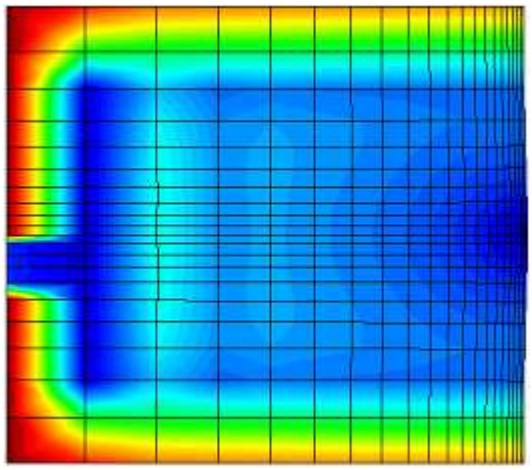

7e

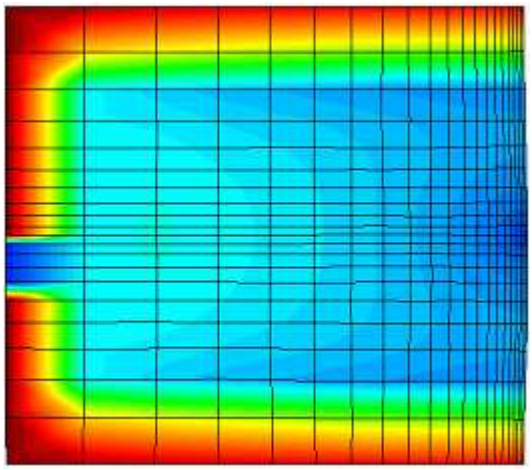

7e'

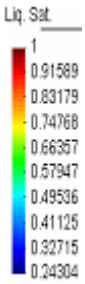

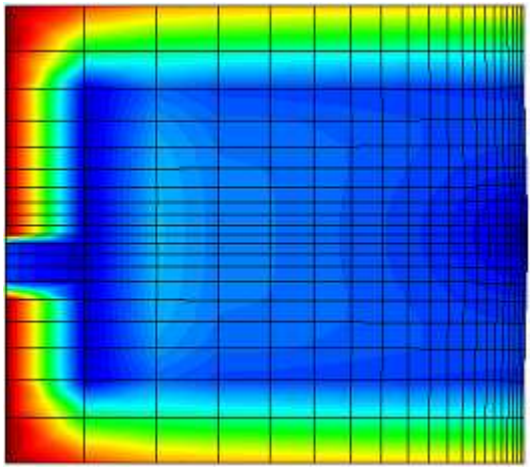

7f

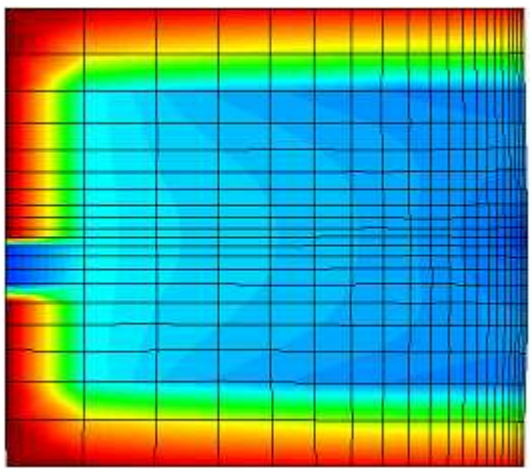

7f'

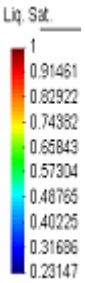

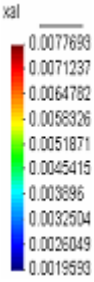

Fig.7 Plotted simulated results of liquid saturation at the time points of 1 year, 5 years, 10 years, 20 years, 50 years and 100 years after CO2 injected as ideal gas (the first) and as real fluid (the second).

Dissolved gas in liquid

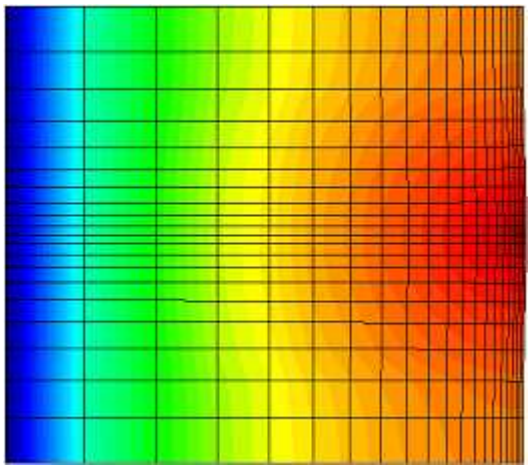

8a

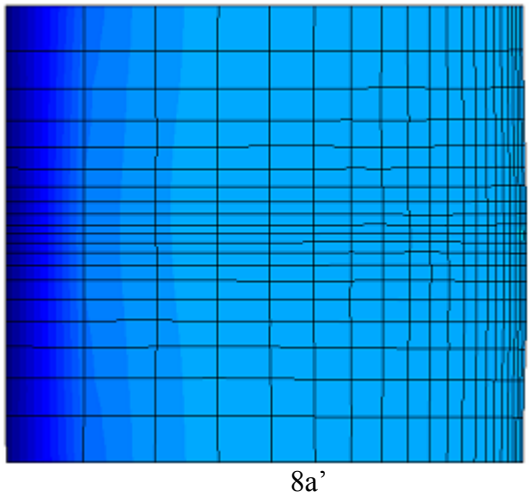

8a'

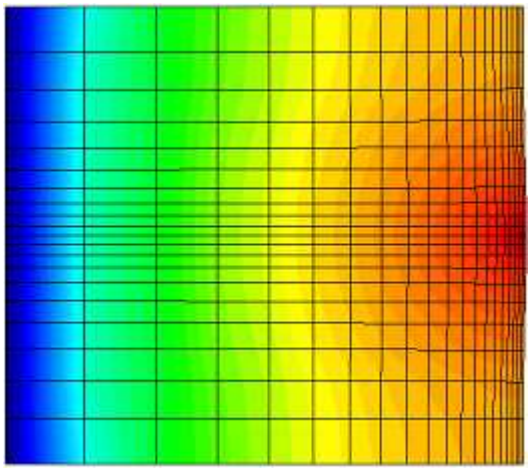

8b

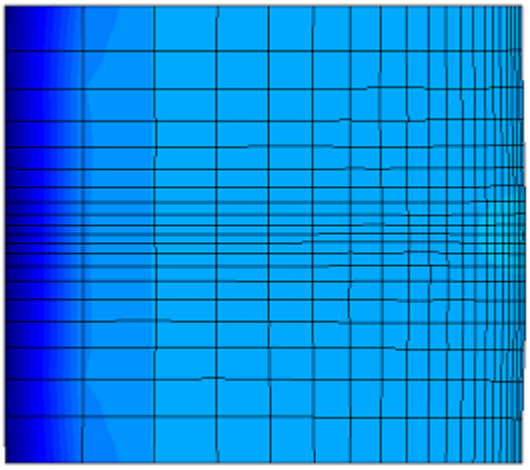

8b'

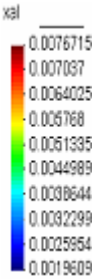

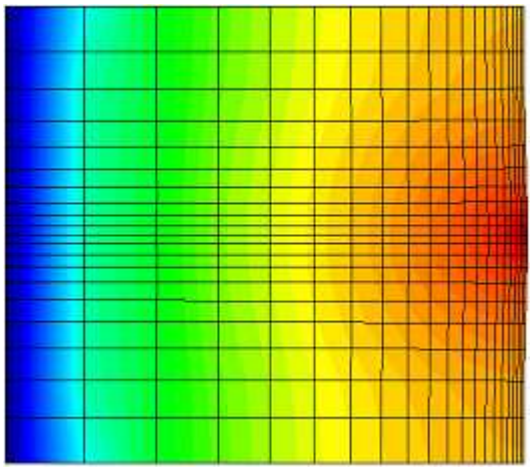

8c

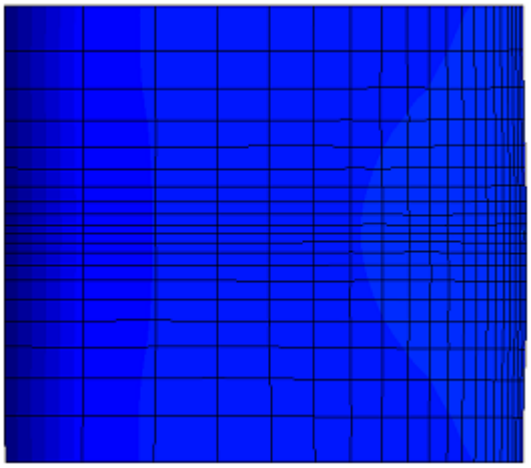

8d’

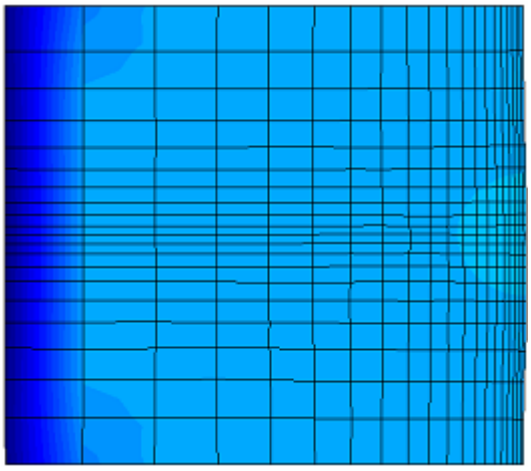

8c’

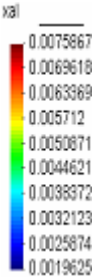

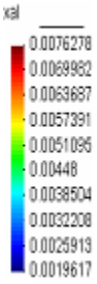

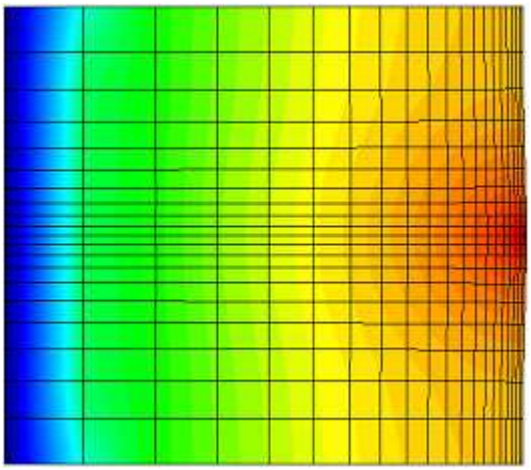

8e

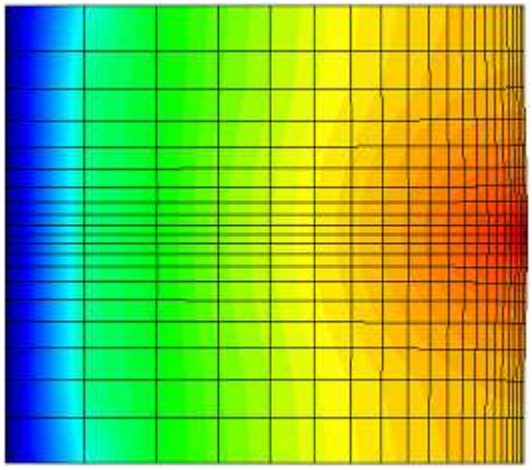

8d

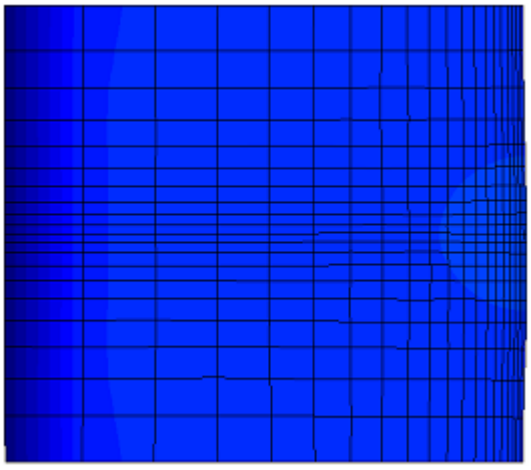

8e’

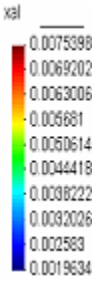

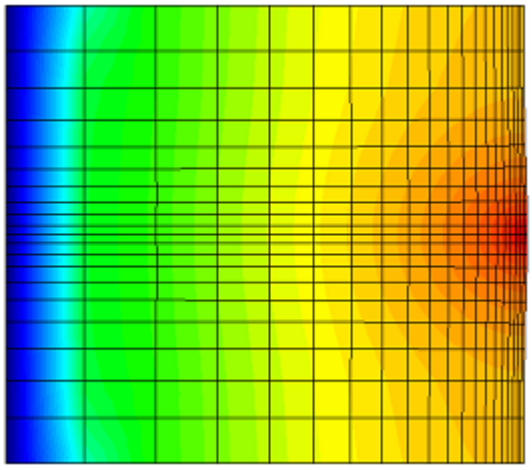

8f

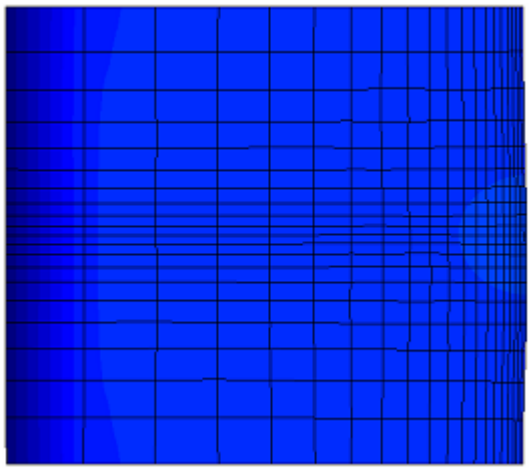

8f'

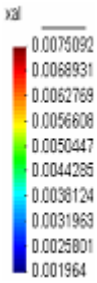

Displacements

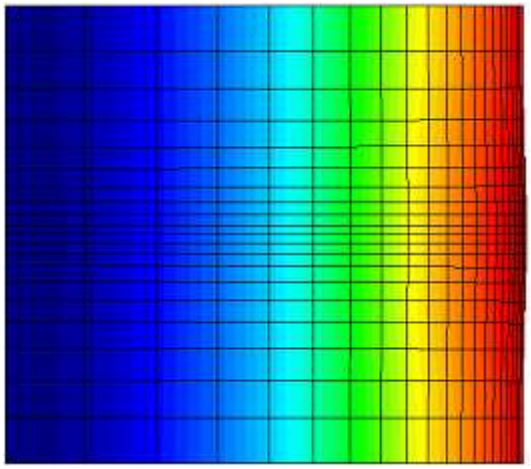

9a

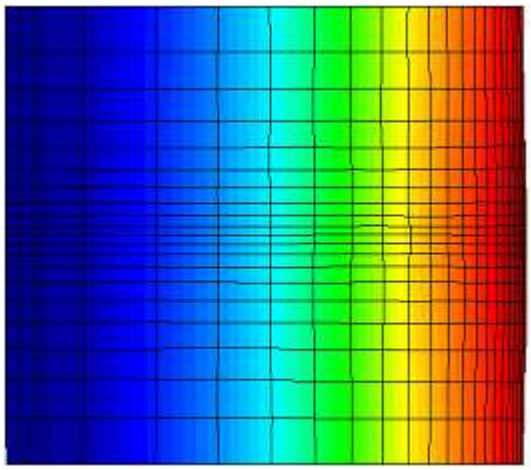

9a'

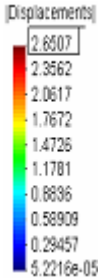

Fig.8 Plotted simulated results of dissolved gas in the liquid (mol) at the time points of 1 year, 5 years, 10 years, 20 years, 50 years and 100 years after CO2 injected as ideal gas (the first) and as real fluid (the second).

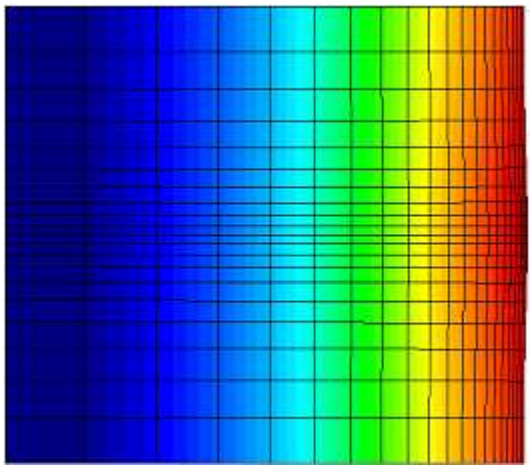

9b

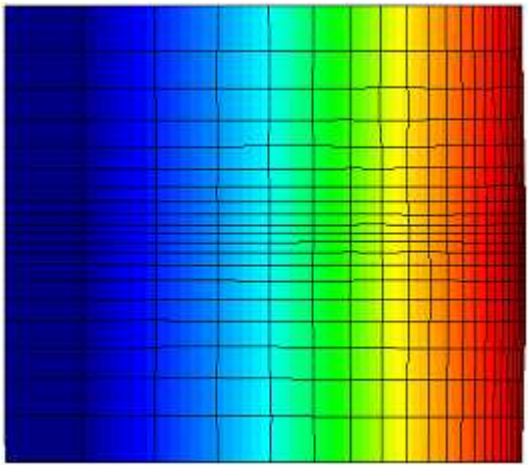

9c’

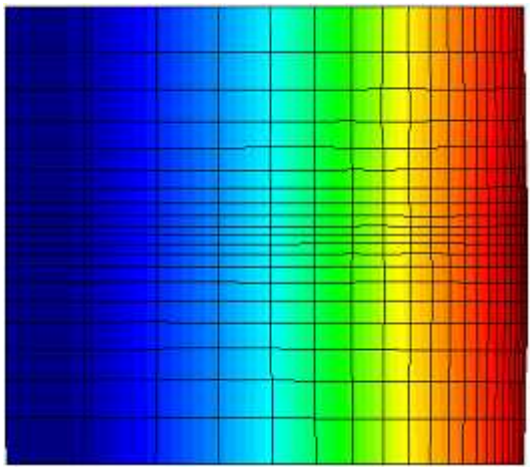

9b’

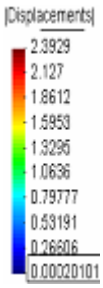

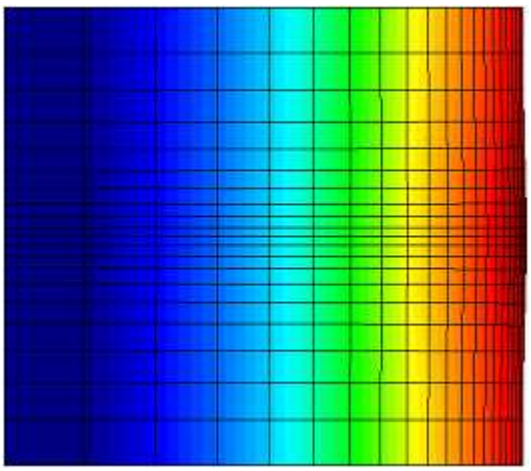

9d

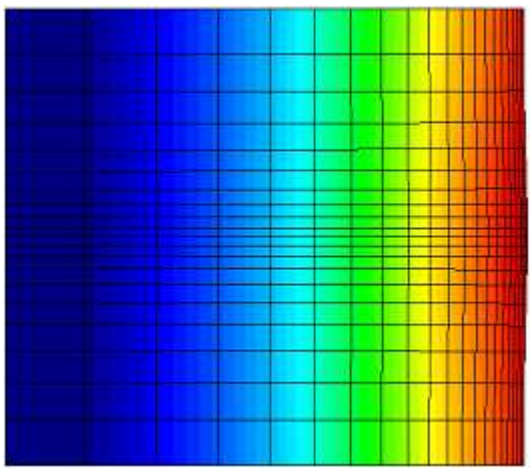

9c

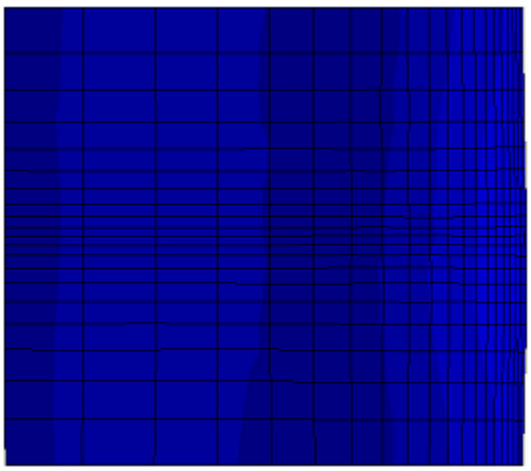

9d’

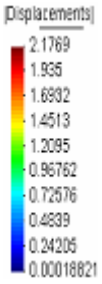

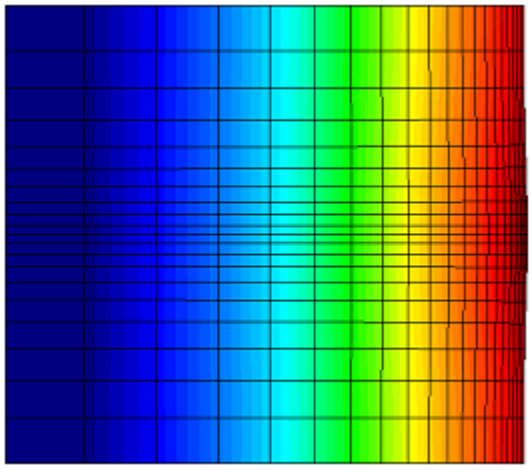

9e

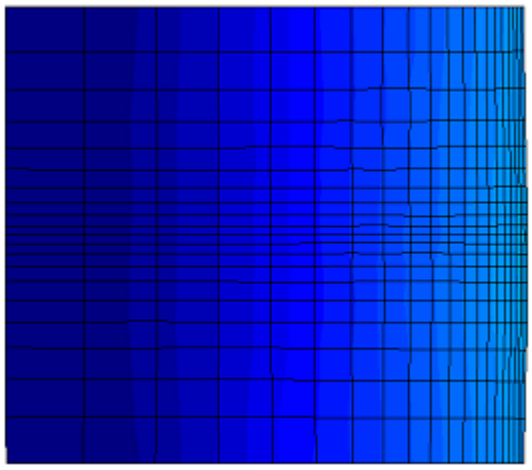

9e’

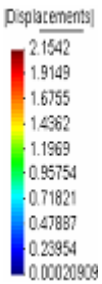

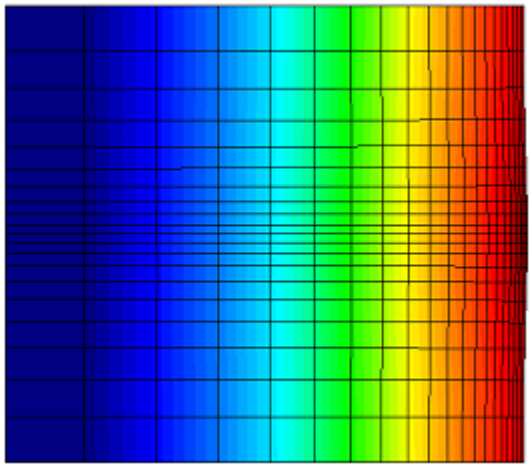

9f

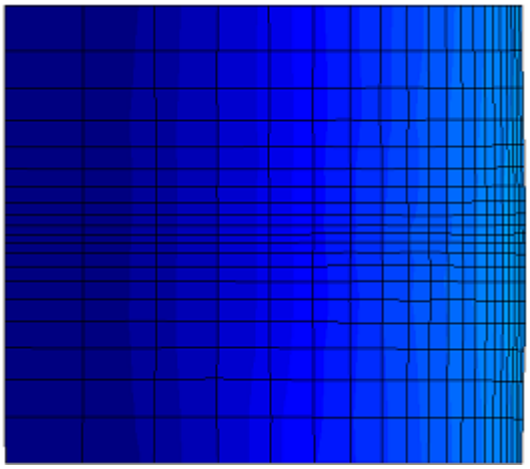

9f’

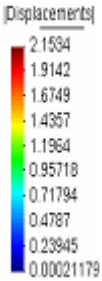

Fig.9 Plotted simulated results of displacements (m) on the geometry at the time points of 1 year, 5 years, 10 years, 20 years, 50 years and 100 years after CO2 injected as ideal gas (the first) and as real fluid (the second).

PH values

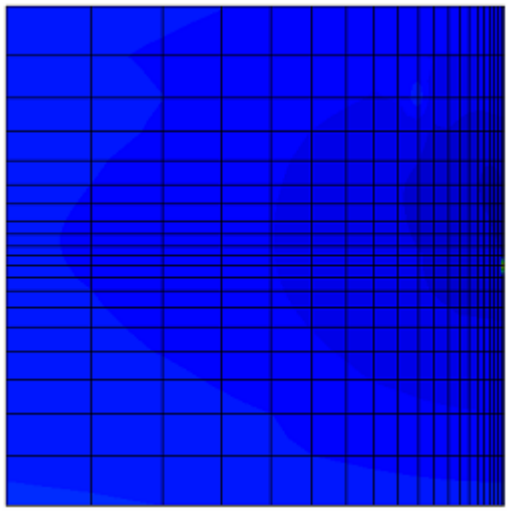

10a

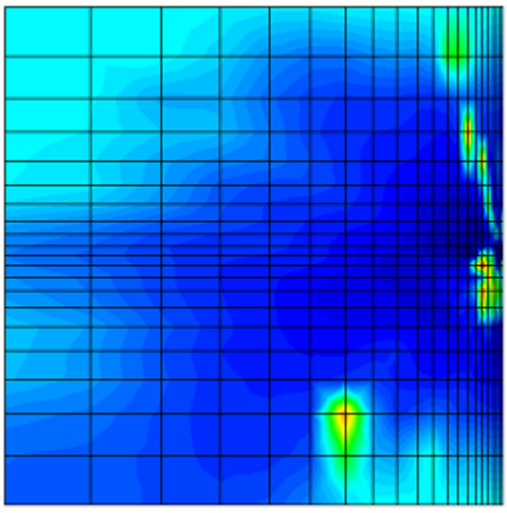

10a'

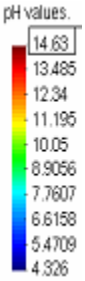

Fig.10 Plotted simulated results of pH values at the time points of 1 year, 5 years, 10 years, 20 years, 50 years and 100 years after CO2 injected as ideal gas (the first) and as real fluid (the second).